Set1 regulates telomere function via H3K4 methylation–dependent and -independent pathways and calibrates the abundance of telomere maintenance factors

Meagan Jezek[a], Winny Sun[a], Maraki Y. Negesse[a], Zachary M. Smith[a], Alexander Orosz[a], and Erin M. Green[a,b,*]

[a]Department of Biological Sciences, University of Maryland Baltimore County, Baltimore, MD 21250; [b]Marlene and Stewart Greenebaum Comprehensive Cancer Center, University of Maryland School of Medicine, Baltimore, MD 21201

ABSTRACT Set1 is an H3K4 methyltransferase that comprises the catalytic subunit of the COMPASS complex and has been implicated in transcription, DNA repair, cell cycle control, and numerous other genomic functions. Set1 also promotes proper telomere maintenance, as cells lacking Set1 have short telomeres and disrupted subtelomeric gene repression; however, the precise role for Set1 in these processes has not been fully defined. In this study, we have tested mutants of Set1 and the COMPASS complex that differentially alter H3K4 methylation status, and we have attempted to separate catalytic and noncatalytic functions of Set1. Our data reveal that Set1-dependent subtelomeric gene repression relies on its catalytic activity toward H3K4, whereas telomere length is regulated by Set1 catalytic activity but likely independent of the H3K4 substrate. Furthermore, we uncover a role for Set1 in calibrating the abundance of critical telomere maintenance proteins, including components of the telomerase holoenzyme and members of the telomere capping CST (Cdc13-Stn1-Ten1) complex, through both transcriptional and posttranscriptional pathways. Altogether, our data provide new insights into the H3K4 methylation–dependent and -independent roles for Set1 in telomere maintenance in yeast and shed light on possible roles for Set1-related methyltransferases in other systems.

Monitoring Editor
Tom Misteli
National Institutes of Health, NCI

Received: Jun 15, 2022
Revised: Oct 5, 2022
Accepted: Nov 17, 2022

INTRODUCTION

As the catalytic component of the COMPASS complex, the methyltransferase Set1 deposits mono-, di-, and trimethylation onto histone H3 lysine 4 (Miller *et al.*, 2001; Roguev *et al.*, 2001; Krogan *et al.*, 2002; Nagy *et al.*, 2002). In yeast, H3K4me3, me2, and me1 are found at gene promoters, gene bodies, and 3′ regions of actively transcribed genes, respectively (Bernstein *et al.*, 2002; Santos-Rosa *et al.*, 2002; Pokholok *et al.*, 2005). Interestingly, in the absence of Set1, genome-wide gene expression analyses have shown that the majority of differentially expressed genes are up-regulated (Venkatasubrahmanyam *et al.*, 2007; Lenstra *et al.*, 2011; Margaritis *et al.*, 2012; Weiner *et al.*, 2012; Jaiswal *et al.*, 2017; Jezek *et al.*, 2017a), indicating that a primary outcome of depleted Set1 and H3K4 methylation is gene derepression or activation. The genes that rely on Set1 for repression are predominantly lowly expressed and are found in genomic regions with limited transcriptional activity, such as Ty elements, ribosomal DNA, meiotic differentiation genes, and telomeres (Nislow *et al.*, 1997; Briggs *et al.*, 2001; Bryk *et al.*, 2002; Berretta *et al.*, 2008; Castelnuovo *et al.*, 2014; Jaiswal *et al.*, 2017).

One of the earliest described phenotypes in yeast cells lacking Set1 was the loss of subtelomeric gene silencing (Nislow *et al.*, 1997;

This article was published online ahead of print in MBoC in Press (http://www.molbiolcell.org/cgi/doi/10.1091/mbc.E22-06-0213) on November 23, 2022.

Conflict of interest: The authors declare that they have no conflicts of interest with the contents of this research article.

*Address correspondence to: Erin M. Green (egreen@umbc.edu).

Abbreviations used: chIP, chromatin immunoprecipitation; CST, Cdc13-Stn1-Ten1 complex; DDR, DNA damage resposne; EV, empty vector; HDAC, histone deacetylase; HU, hydroxyurea; me, methyl; NMD, nonsense mediated decay; ORF, open reading frame; RRM, RNA recognition motif; RT-qPCR, reverse transcription quantitative polymerase chain reaction; SC, synthetic complete; SDS–PAGE, sodium dodecyl-sulfate polyacrylamide gel electrophoresis; SIR, silent information regulator; TEL, telomere; Ub, ubiqtuin; YPD, yeast extract, peptdone, dextrose.

Corda *et al.*, 1999; Krogan *et al.*, 2002). *set1*Δ cells also have short telomeres and disrupted telomere clustering at the nuclear periphery (Nislow *et al.*, 1997; Krogan *et al.*, 2002; Schneider *et al.*, 2005; Trelles-Sticken *et al.*, 2005). Given the low levels of H3K4 methylation at telomeric regions, it was proposed that Set1 indirectly regulates subtelomeric gene silencing, and likely telomere length, through euchromatic H3K4me3, which is thought to prevent redistribution of the silencing protein Sir2, the histone deacetylase (HDAC) of the SIR complex, from subtelomeres to internal chromosomal sites (Santos-Rosa *et al.*, 2004; Venkatasubrahmanyam *et al.*, 2007). However, subsequent chromatin immunoprecipitation and genetic studies indicate that subtelomeric gene repression by Set1 predominantly occurs through a SIR-independent mechanism (Ng *et al.*, 2003; Leung *et al.*, 2011; Margaritis *et al.*, 2012; Jezek *et al.*, 2017a). These observations are consistent with recent understanding of SIR-mediated silencing at subtelomeres, which revealed largely noncontiguous subtelomeric regions reliant on the SIR complex for silencing, whereas Set1 appears to promote silencing in larger, contiguous regions and at a higher number of subtelomeres (Ellahi *et al.*, 2015; Jezek *et al.*, 2017a). These observations indicate that the precise role for Set1 in maintaining functional telomere-linked properties such as gene repression, telomere length, and nuclear position remains obscure. Interestingly, in previous work, our lab has shown that the *set1*Δ transcriptome is highly similar to mutants lacking telomere maintenance factors, particularly the telomerase subunit, Est3 (Jezek *et al.*, 2017a). This further suggests that Set1 may have a more direct role in telomere regulation than previously appreciated.

Although most known functions of Set1 have been attributed to methylation of H3K4, there is growing evidence for H3K4me-independent functions for Set1. For example, two other substrates have been described for Set1: the kinetochore protein, Dam1 (Zhang *et al.*, 2005), and another histone modification at H3K37, where Set1 promotes methylation with Set2 (Santos-Rosa *et al.*, 2021). Although not extensively documented for yeast Set1, some orthologues of Set1 have been demonstrated to perform noncatalytic functions as well (Kirmizis *et al.*, 2007; Dorighi *et al.*, 2017; Rickels *et al.*, 2017, 2020). The discovery of these additional substrates and functions implicates Set1 in genome regulation roles separate from its H3K4 methyltransferase activity.

In wild-type cells, multiple protein complexes bind telomere ends and coordinate telomere capping and elongation. These include the Cdc13-Stn1-Ten1 (CST) capping complex and telomerase, composed of the catalytic subunit Est2, regulatory subunits Est1 and Est3, and the RNA component *TLC1* (Wellinger and Zakian, 2012; Kupiec, 2014; Jezek and Green, 2019). These and other proteins are critical to telomere health, and numerous mechanisms appear to control their precise abundance in cells. This includes cell cycle–regulated transcription of genes encoding telomerase and CST subunits, ribosomal frameshifting and nonsense-mediated decay to control translation, and posttranslational regulation including control of protein degradation via phosphorylation (Morris and Lundblad, 1997; Enomoto *et al.*, 2004; Larose *et al.*, 2007; Tuzon *et al.*, 2011; Advani *et al.*, 2013; Holstein *et al.*, 2014; Liu *et al.*, 2014; Tucey and Lundblad, 2014; Cesena *et al.*, 2017; Gopalakrishnan *et al.*, 2017; Mersaoui and Wellinger, 2019; Garcia *et al.*, 2020). These studies have revealed that changes in their stoichiometry alter telomere length and stability, indicating that a precise and well-defined balance of telomerase and CST components is critical to telomere maintenance.

In this study, we assayed mutations in Set1, the COMPASS complex, and at H3K4 to assess the specific contribution of H3K4 methylation by Set1 to subtelomeric gene repression and telomere length maintenance. Our data indicate that the catalytic core of Set1 is required for its role in both gene repression and telomere length; however, there are likely H3K4 methyl–independent mechanisms required for the regulation of telomere length. Furthermore, our data identify a role for Set1 and H3K4 methylation in modulating the abundance of telomere maintenance proteins, including components of telomerase and the CST complex, through both transcriptional and posttranscriptional pathways. Altogether, these data provide new insights into how Set1 contributes to telomere maintenance and are likely applicable to related proteins in other organisms.

RESULTS

The Set1 SET domain maintains telomere length and subtelomeric gene repression

In the absence of Set1, cells display a number of telomere-related defects (Nislow *et al.*, 1997; Corda *et al.*, 1999; Krogan *et al.*, 2002; Schneider *et al.*, 2005; Trelles-Sticken *et al.*, 2005; Jezek *et al.*, 2017a), including loss of subtelomeric gene repression as demonstrated by derepression of *TEL07L*-adjacent genes *COS12* and *YGL262W* (Figure 1A) and short telomeres (Figure 1B). In investigating other telomere-related phenotypes of *set1*Δ cells, we also observed a faster rate of senescence in cells lacking Set1 and the telomerase component *TLC1*, as compared with *tlc1*Δ single mutants (Figure 1C). These data show that the telomeres in *set1*Δ *tlc1*Δ cells are shortened critically to reach a crisis point, prompting cellular senescence. The *set1*Δ *tlc1*Δ cells are able to recover, however, and form survivors through a telomerase-independent mechanism, albeit at a slower rate than *tlc1*Δ cells (Figure 1C). We also found that loss of Set1 exacerbates the growth defect of cells carrying a temperature-sensitive allele of *CDC13*, which encodes a member of the CST telomere capping complex (Figure 1D). While *cdc13-1* cells show almost no growth at 30°C and some growth at 26°C, the *set1*Δ *cdc13-1* mutants grow much more poorly at 26 and 27°C compared with either single mutant, indicating that Set1 functions in a pathway related to that of Cdc13. This is consistent with our previous observations indicating a broader role for Set1 in telomere maintenance pathways (Jezek *et al.*, 2017a), rather than a targeted function in controlling subtelomeric gene silencing.

To better define the molecular contribution of Set1 in preventing telomere-related defects, we monitored subtelomeric silencing and telomere length in mutants specifically lacking H3K4 methylation by carrying an allele expressing the *H3K4R* mutant as the sole copy of an H3-encoding gene. These cells showed derepression of subtelomeric genes similar to that of *set1*Δ cells (Figure 2A) and also a similar shortening in telomere length (Figure 2B). We combined the *H3K4R* mutant with *set1*Δ and also observed that the subtelomeric gene repression and telomere length were reduced to similar extents in the double mutant compared with both single mutants (Figure 2, A and B). While this suggests an epistatic interaction between *SET1* and *H3K4*, as is expected based on their biochemical relationship, previous work has demonstrated that the Set1 protein is destabilized in the absence of H3K4 methylation in these mutants due to an autoregulatory feedback mechanism (Soares *et al.*, 2014). In addition, the decreased dosage of histones in these strains is likely to modify *set1*Δ phenotypes, as demonstrated previously (de La Roche Saint-André and Géli, 2021), indicating that it is challenging to conclusively determine the relationship between Set1 and H3K4 methylation using these strains. We therefore used another approach to address whether the methyltransferase activity of Set1 is required for subtelomeric gene repression and telomere length maintenance by generating multiple catalytically inactive mutations of Set1. We used cells expressing *FLAG-SET1* from a plasmid under

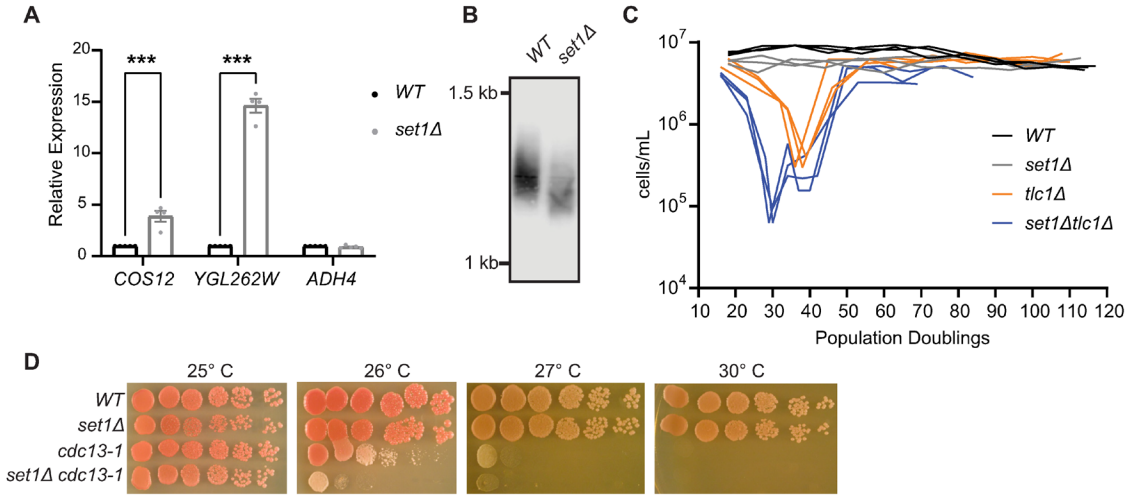

FIGURE 1: Loss of Set1 is linked to telomere defects. (A) RT-qPCR analysis of *TEL07L* genes (*COS12*, *YGL262W*, and *ADH4*) in wild-type (*WT*; yEG230) and *set1*Δ (yEG232) cells. *ADH4* is farther from the telomere and not subject to repression by Set1. Expression normalized to the control gene *TFC1* and relative to *WT* is shown. Error bars represent SEM for a minimum of three biological replicates. Significance was evaluated using two-way ANOVA and Tukey's multiple comparisons test. *P* values are indicated as follows: *** < 0.001. (B) Southern blot showing terminal telomere fragment molecular weight in *WT* (yEG230) and *set1*Δ (yEG232) cells. The terminal telomere fragments were recognized with probe 5′-biotin-CACACCCACACCCACACC-3′. (C) Senescence rate of *WT*, *set1*Δ, *tlc1*Δ, and *set1*Δ *tlc1*Δ cells, which originated from tetrad dissection of yEG880. At each time point, population doublings were calculated based on the cell density. Three biological replicates are shown. (D) Fivefold serial dilutions of saturated cultures of the indicated strains were spotted on YPD and incubated at different temperatures before imaging. *WT* (DLY3001), *set1*Δ (yEG1296), *cdc13-1* (DLY4557/yEG1297), and *set1*Δ *cdc13-1* (yEG1298). All yeast strains described in this figure are derived from the BY4741 background, except in panel D, which are W303.

the control of the *SET1* promoter in *set1*Δ cells and generated the *H1017L*, *C1019A*, and *G951S* mutants (Nislow *et al.*, 1997; Schlichter and Cairns, 2005; Ramakrishnan *et al.*, 2016; Cruz *et al.*, 2018). While we did observe complete loss of H3K4 methylation in these mutants, we also found that their steady-state protein levels were much lower than wild-type FLAG-Set1 (Figure 2D), as previously shown for some catalytically inactive mutants (Soares *et al.*, 2014). As expected, the mutants all showed derepression of subtelomeric genes at *TEL07L* and *TEL09R* (Figure 2E and Supplemental Figure S1, A and B), largely similar to *set1*Δ cells carrying an empty vector. In addition, these strains showed short telomeres (Figure 2F), similar to or even shorter than complete loss of Set1. While these data may indicate that Set1 catalytic activity is the primary requirement to support telomere maintenance, the decreased stability of Set1 with these mutations leaves open the possibility that alternate, noncatalytic functions for Set1 may be required. Furthermore, these data underscore the importance of evaluating protein expression of methyltransferases when using mutants to distinguish catalytic and noncatalytic roles.

Set1 contains two RNA recognition motifs (RRM1 and RRM2) near the N-terminus that predominantly bind mRNAs, as well as a small number of noncoding RNAs (Trésaugues *et al.*, 2006; Luciano *et al.*, 2017; Sayou *et al.*, 2017), and the catalytic core of Set1 is composed of the N-SET, SET, and post-SET domains near the C-terminus of the protein (Figure 3A). To determine whether noncatalytic functions of Set1 contribute to its role at telomeres, we generated deletions of RRM1, RRM2, and a region spanning all of RRM1 and RRM2 (RRM1-2) in the *FLAG-SET1* construct (Figure 3A). Previous work (Schlichter and Cairns, 2005; Trésaugues *et al.*, 2006; Luciano *et al.*, 2017) demonstrated that the absence of the RRM domains reduces H3K4me3 levels. Therefore, we also generated the reported hyperactive methylation mutant G990E (Schlichter and Cairns, 2005) to help overcome this deficiency and potentially separate H3K4 methyltransferase activity from RNA binding activity. In addition, we tested the H422A point mutation, which is reported to block RNA binding by RRM2 yet maintain H3K4 methylation status. Immunoblotting of the FLAG-Set1 ΔRRM1, ΔRRM2, and ΔRRM1-2 proteins expressed from their endogenous promoter, as well as the H422A point mutant, showed expression similar to that of wild-type FLAG-Set1 for all mutant proteins (Figure 3B and Supplemental Figure S2A). H3K4 methylation levels were also comparable to that in cells with FLAG-Set1, although some degree of H3K4me3 was lost in these mutants, even in combination with the *G990E* allele (Figure 3C and Supplemental Figure S2B). This is likely due to the reported reduction in Set1 chromatin binding when the RRMs are absent (Sayou *et al.*, 2017).

Analysis of subtelomeric gene expression using reverse transcription–quantitative PCR (RT-qPCR) showed that the RNA binding activity of Set1 is not the primary contributor to gene repression, as the mutants largely maintained repression of *TEL07L* and *TEL09R* subtelomeric genes, with only mild derepression observed in ΔRRM1 and ΔRRM2 strains (Figure 3D). Loss of RNA binding by Set1 also appears to minimally affect telomere length, as the H422A mutant and RRM-deleted proteins (ΔRRM1, ΔRRM2, and ΔRRM1-2) displayed telomere lengths more similar to those of wild-type than *set1*Δ cells (Figure 3E). Similar assays using the FLAG-Set1 RRM-deleted protein combined with the hyperactive G990E mutation were performed; however, there was no change in phenotype in the presence of this mutation (Supplemental Figure S2, C and D).

We next tested whether FLAG-Set1 containing only the catalytic core, residues 762–1081 (Δ1-761) (Kim *et al.*, 2013), was sufficient to promote subtelomeric gene repression and telomere length maintenance. As demonstrated in previous work (Kim *et al.*, 2013), FLAG-Set1 Δ1-761 is stable, highly expressed, and maintains wild-type

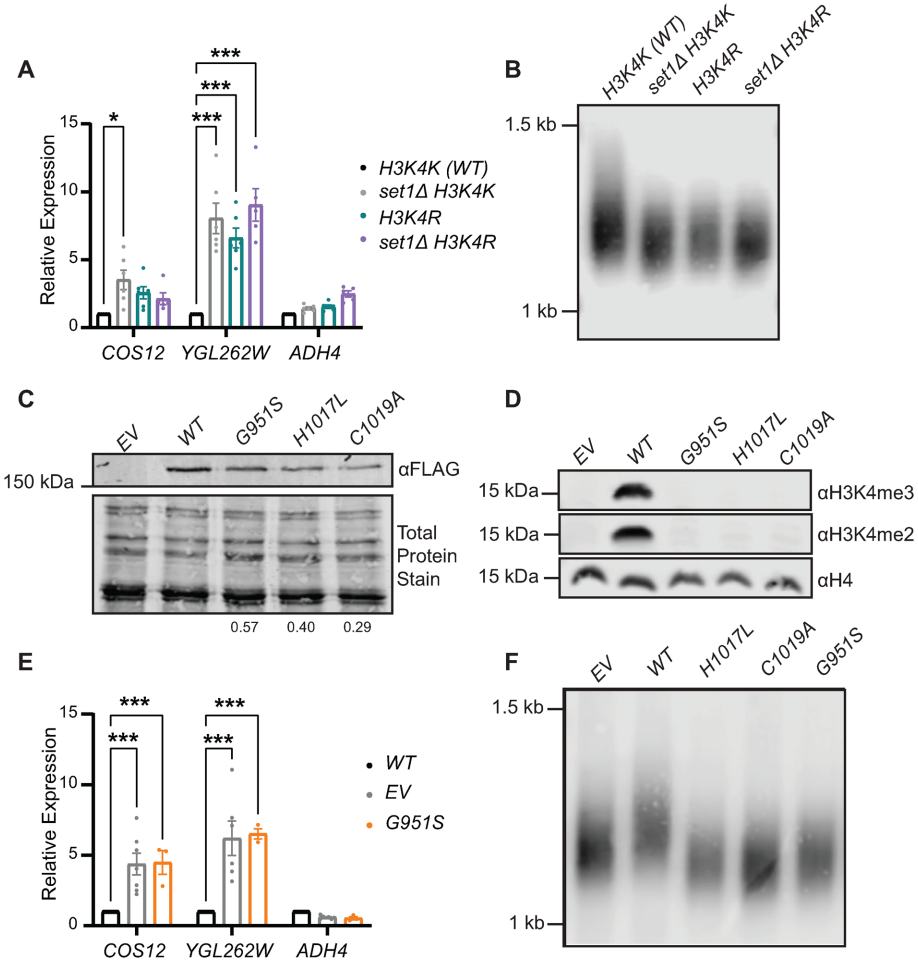

FIGURE 2: Analysis of catalytic requirements of Set1 in subtelomeric gene repression and telomere length control. (A) RT-qPCR analysis of *TEL07L* genes in *WT H3K4K* (yEG108), *set1Δ H3K4K* (yEG1342), *H3K4R* (yEG109), and *set1Δ H3K4R* (yEG1343) cells, derivatives of the histone shuffle strain WZY42, which is the S288C background (Zhang *et al.*, 1998). Expression was normalized to the control gene *TFC1* and is shown relative to *WT*. Error bars represent SEM for a minimum of three biological replicates. (B) Southern blot showing terminal telomere fragments in yeast strains described for panel A. (C, D) Western blots depicting FLAG-Set1 levels (C) and H3K4 methylation (D) in *set1Δ* (yEG232) cells expressing *FLAG-SET1* (yEG738), with catalytic mutations *G951S* (yEG984), *H1017L* (yEG885), and *C1019A* (yEG886) or an empty vector (EV; yEG647). In panel C, the abundance of each Set1 mutant relative to that of wild type was determined relative to total protein by image analysis (see *Materials and Methods*) and is indicated in text below the gel. (E) RT-qPCR analysis of *TEL07L* genes in *set1Δ* cells carrying an empty vector (EV) (yEG647) or expressing FLAG-Set1 (*WT*; yEG738) or FLAG-Set1 G951S (yEG984). Expression was normalized to the control gene *TFC1* and is shown relative to *WT*. Error bars represent SEM for a minimum of three biological replicates. (F) Southern blot showing terminal telomere fragment molecular weight in *set1Δ* cells with empty vector (EV; yEG647), *WT* FLAG-Set1 (yEG738), or FLAG-Set1 catalytic mutants *G951S* (yEG984), *H1017L* (yEG885), and *C1019A* (yEG886). For gene expression analysis, significance was evaluated using two-way ANOVA and Tukey's multiple comparisons test. *P* values are indicated as follows: * < 0.05, *** < 0.001. All yeast strains described in this figure are derived from the S288C/BY4741 backgrounds.

H3K4me levels (Figure 3, B and C). Cells expressing FLAG-Set1 Δ1-761 closely mimicked the subtelomeric gene expression of cells containing full-length FLAG-Set1 (Figure 3D) and largely rescued the defect in telomere length, with only a modest decrease in length compared with wild-type cells (Figure 3E). These data indicate that the catalytic core of Set1 is sufficient to maintain subtelomeric gene repression and mostly maintains telomere length as well. These results are consistent with previous work indicating that overexpression of the SET domain of Set1 rescues the telomere position effect phenotype of *set1Δ* cells (Nislow *et al.*, 1997; Corda *et al.*, 1999).

Set1 has also been implicated in DNA damage response (DDR) pathways (Corda *et al.*, 1999; Faucher and Wellinger, 2010). To determine whether Set1's role in these pathways is also primarily dependent on the SET domain, we tested growth of strains expressing mutant FLAG-Set1 in the presence of hydroxyurea (HU) and caffeine (Supplemental Figure S3). Cells lacking Set1 (empty vector) grew poorly in the presence of either HU or caffeine, whereas the expression of FLAG-Set1 was able to rescue this growth defect. The growth of RNA binding mutants of FLAG-Set1 (ΔRRM1, ΔRRM2, ΔRRM1-2, and H422A) were similar to that of wild type, whereas the catalytic mutants H1017L, C1019A, and G951S were strongly inhibited in the presence of HU or caffeine (Supplemental Figure S3). Expression of the FLAG-Set1 Δ1-761 catalytic core exhibited growth similar to that of full-length FLAG-Set1, indicating that the catalytic core is also sufficient for Set1's role in the DDR pathway (de La Roche Saint-André and Géli, 2021).

Subtelomeric gene repression, but not telomere length maintenance, depends on H3K4 methylation

In addition to Set1, COMPASS complex subunits and the Rad6-Bre1 H2B ubiquitin ligase complex promote H3K4 methylation: loss of COMPASS subunits Spp1 and Sdc1 leads to a reduction in H3K4me3 and H3K4me2, respectively (Dehé *et al.*, 2006), and *rad6Δ* mutants have no H3K4me due to the requirement for H2BK123Ub (Sun and Allis, 2002; Dehé *et al.*, 2005). We and others have previously shown that subtelomeric gene repression of *TEL07L* adjacent genes *COS12* and *YGL262W* is reduced in *spp1Δ* and *sdc1Δ* mutants (Figure 4A; Miller *et al.*, 2001; Jaiswal *et al.*, 2017; Jezek *et al.*, 2017a). However, there is less derepression in these cells compared with those lacking Set1, indicating a partial requirement for these COMPASS complex components in subtelomeric gene repression. We also monitored subtelomeric gene expression in *rad6Δ* cells, which have no H3K4 methylation, and observed that this mutant closely mimics the derepression observed in *set1Δ* cells (Figure 4A). In Southern blots of terminal telomere fragments, both *spp1Δ* and *sdc1Δ* mutants showed little defect in telomere length compared with isogenic wild-type cells (Figure 4B). Similarly, there is some defect in telomere length in the *rad6Δ* mutant compared with wild type (Figure 4B; Leung *et al.*, 2011; Wu *et al.*, 2017), despite the clear loss of subtelomeric gene repression in

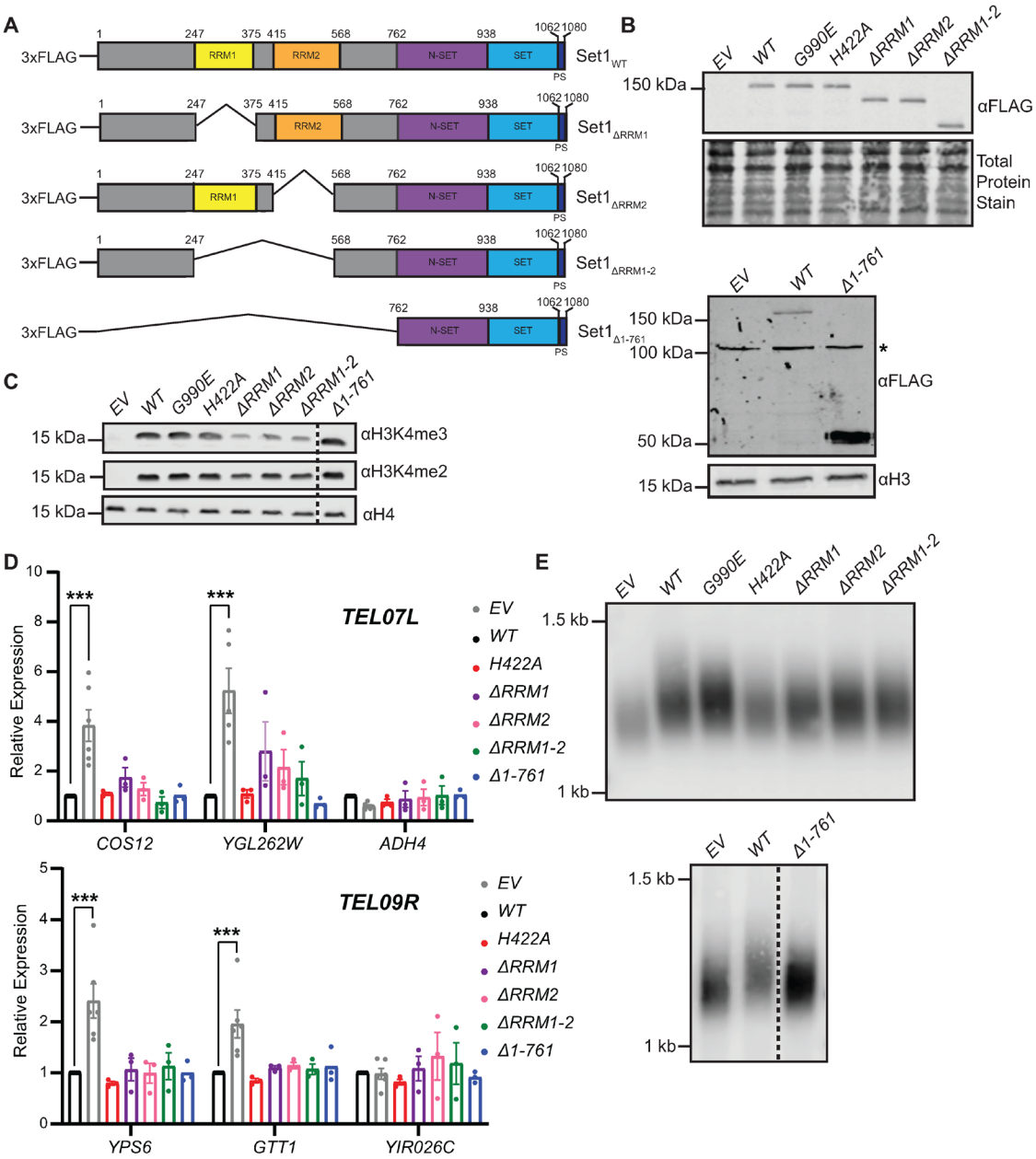

FIGURE 3: The catalytic core of Set1, but not the RRM domains, is required for subtelomeric gene repression and telomere length maintenance. (A) Schematic depicting wild-type Set1 domain structure (top) and domain deletions (Δ*RRM1*, Δ*RRM2*, Δ*RRM1-2*) and C-terminal truncation (Δ*1-761*) used in expression vectors with an N-terminal FLAG tag in *set1*Δ cells. (B) Western blots of yeast whole cell extracts probed with anti-FLAG showing levels of wild-type (yEG738) and mutant FLAG-Set1 expressed in *set1*Δ cells (EV, yEG647; *G990E*, yEG740; *H422A*, yEG741; Δ*RRM1*, yEG746; Δ*RRM2*, yEG747; Δ*RRM1-2*, yEG748; Δ*1-761*, yEG1102) and (C) H3K4me3 and H3K4me2 levels for each strain expressing FLAG-Set1 variants. Total protein stain, anti-H3, or anti-H4 was used as loading controls. Asterisk (*) indicates a nonspecific band detected by the anti-FLAG antibody. (D) RT-qPCR analysis of *TEL07L* genes in *set1*Δ cells carrying an empty vector (EV) or expressing FLAG-Set1 (*WT*) or FLAG-Set1 mutants (strains as described in panel B). Expression was normalized to the control gene *TFC1* and is shown relative to *WT*. Error bars represent SEM for a minimum of three biological replicates. Significance was evaluated using two-way ANOVA and Dunnett's multiple comparisons test. *P* values are indicated as follows: *** < 0.001. (E) Southern blot showing terminal telomere fragment molecular weight in *set1*Δ cells with empty vector (EV) or FLAG-Set1 mutants (strains as described in panel B). In all gel image panels, the dashed line separates samples run on the same gel in which intervening lanes were removed for clarity. All yeast strains described in this figure are derived from the BY4741 background.

these cells. These data support the possibility that defects in telomere length maintenance and subtelomeric gene expression can be separated in some mutants lacking H3K4 methylation. Furthermore, while our data indicate a requirement for the catalytic core of Set1 in telomere maintenance phenotypes, there appears to be only a partial requirement for H3K4 methylation, particularly for telomere length, which shows regulation independent of Spp1, Sdc1, and Rad6.

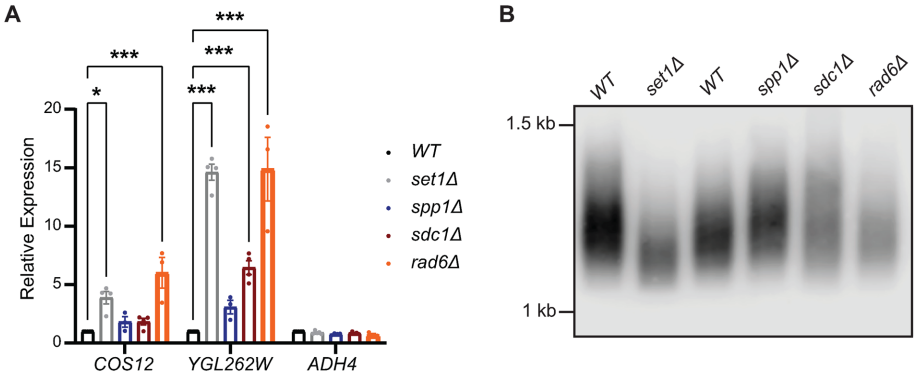

FIGURE 4: The requirement for other COMPASS components and Rad6 in subtelomeric gene repression and telomere length. (A) RT-qPCR analysis of *TEL07L* genes in *WT* (yEG230), *set1*Δ (yEG230), *spp1*Δ (yEG100), *sdc1*Δ (yEG110), and *rad6*Δ (yEG623). Expression was normalized to the control gene *TFC1* and is shown relative to *WT*. Error bars represent SEM for a minimum of three biological replicates. Significance was evaluated using two-way ANOVA and Dunnett's multiple comparisons test. *P* values are indicated as follows: * < 0.05, *** < 0.001. (B) Southern blot showing terminal telomere fragment molecular weight in *WT* (yEG230), *set1*Δ (yEG232), *WT* (yEG001), *spp1*Δ (yEG100), *sdc1*Δ (yEG110), and *rad6*Δ (yEG623). All yeast strains described in this figure are derived from the BY4741 background.

The abundance of telomere maintenance factors is altered upon loss of Set1

Next, we sought to better define the potential roles for Set1 in telomere length maintenance and subtelomeric gene repression. We and others have previously suggested that Set1 and H3K4 methylation likely support telomere maintenance through additional mechanisms beyond regulating repressive chromatin factors at subtelomeres (Margaritis *et al.*, 2012; Jezek *et al.*, 2017a). This observation is also supported by our finding that the transcriptome of *set1*Δ mutants is highly correlated with the transcriptome of yeast cells lacking components of the telomerase holoenzyme, such as *est1*Δ, *est3*Δ, and *tlc1*Δ, as well as mutants in other telomere maintenance pathways (Jezek *et al.*, 2017a).

To determine whether any telomere maintenance factors are misregulated in the absence of Set1, we assayed mRNA levels of a subset of relevant genes in *set1*Δ cells using RT-qPCR (Figure 5A). In these mutants, members of the CST capping complex (Cdc13-Stn1-Ten1) showed altered steady-state mRNA levels, with higher levels of *CDC13* and *STN1* mRNAs and lower levels of *TEN1* mRNA. In addition, the mRNAs coding for telomerase subunits *EST1* and *EST2* and the telomerase RNA, *TLC1*, all showed increased abundance in the absence of Set1, whereas the *EST3* mRNA is twofold less abundant. The mRNA abundances of additional telomere maintenance regulators, including those coding for the transcription factor Rap1 and members of the RFA, yKu, and Rif1/2 complexes, were also tested; however, there were few statistically significant changes in mRNA levels in *set1*Δ cells compared with wild type (Figure 5A). The changes in gene expression observed by RT-qPCR were similar to that observed in our previous RNA-seq analysis of *set1*Δ cells (Martín *et al.*, 2014; Jezek *et al.*, 2017a), summarized in the heatmap in Figure 5B. Although the same strain background was used in each experiment, *YKU70* and *YKU80* showed more change in expression in *set1*Δ cells by RNA-seq analysis rather than RT-qPCR; however, the reason for this discrepancy is not known.

We also tested whether mRNA abundance of a subset of telomere maintenance factors is altered in the *spp1*Δ, *sdc1*Δ, and *rad6*Δ mutants (Figure 5C). While some changes in mRNA levels were observed in the *spp1*Δ cells lacking H3K4me3, the *sdc1*Δ mutant most closely resembled *set1*Δ cells, indicating that loss of H3K4me2 is likely a main factor in disrupting the levels of mRNAs encoding telomere maintenance proteins in *set1*Δ cells. The *rad6*Δ mutant showed the most difference from the profile observed in *set1*Δ cells. While this may in part be due to loss of H3K4 methylation, it also likely stems from other functions for Rad6, including its role in promoting H3K79 methylation (Lee *et al.*, 2007; Leung *et al.*, 2011; Wu *et al.*, 2017).

Previous reports indicate that the expression levels and stoichiometry of telomere regulators such as CST and telomerase are highly calibrated by the cell (Morris and Lundblad, 1997; Enomoto *et al.*, 2004; Larose *et al.*, 2007; Tuzon *et al.*, 2011; Advani *et al.*, 2013; Holstein *et al.*, 2014; Liu *et al.*, 2014; Tucey and Lundblad, 2014; Cesena *et al.*, 2017; Gopalakrishnan *et al.*, 2017; Mersaoui and Wellinger, 2019; Garcia *et al.*, 2020). Our analysis of mRNA abundance indicates that the levels of these proteins are likely changing in the absence of Set1. To monitor protein abundance of the CST and telomerase complexes, we epitope tagged CST and telomerase subunits in wild-type and *set1*Δ cells and performed quantitative immunoblotting (Figure 5, D–H). The target protein abundance was monitored using an anti-MYC antibody, and total protein levels were determined by staining the blot with a general protein stain. Cdc13-MYC levels were slightly but significantly reduced in *set1*Δ relative to wild type, and Stn1-MYC protein levels appear to be more reduced in cells lacking Set1, whereas Ten1 levels do not significantly differ in *set1*Δ cells (Figure 5, D–H). Interestingly, the altered abundance of Stn1 protein does not parallel the changes in *STN1* mRNA expression, suggesting that it may be subject to translational or posttranslational control in the absence of Set1.

The telomerase subunit Est1 showed increased protein abundance in *set1*Δ cells, consistent with higher levels of *EST1* mRNA in the mutant (Figure 5, A and G). Intriguingly, our analysis of Est3-MYC protein levels showed only a minor decrease in Est3-MYC abundance in *set1*Δ cells compared with wild type (Figure 5H). This was surprising, given that the *EST3* mRNA abundance was the most substantially decreased in the absence of Set1 (Figure 5A). It was also decreased in the *sdc1*Δ and *rad6*Δ mutants (Figure 5C), and the *H3K4R* mutant showed similarly reduced levels of *EST3* mRNA (Figure 5I), indicating that the abundance of this mRNA is likely dependent on functional Set1 and H3K4 methylation levels.

Regulation of *EST3* mRNA in *set1*Δ mutants

To better understand the relationship between *EST3* mRNA and protein levels, we also evaluated the steady-state levels of the mRNA encoding *EST3-MYC*. This mRNA had equivalent abundances in wild-type and *set1*Δ cells, unlike the endogenous *EST3*; however, its levels were substantially decreased compared with the endogenous mRNA (Supplemental Figure S4A). Currently, immunoblotting of the endogenous protein is not feasible, as there is not an available antibody for the recognition of yeast Est3. Previous reports have indicated that epitope tags disrupt the function of Est3 (Tuzon *et al.*, 2011; Tucey and Lundblad, 2014); therefore, we evaluated the function of our Est3-MYC construct in subtelomeric gene

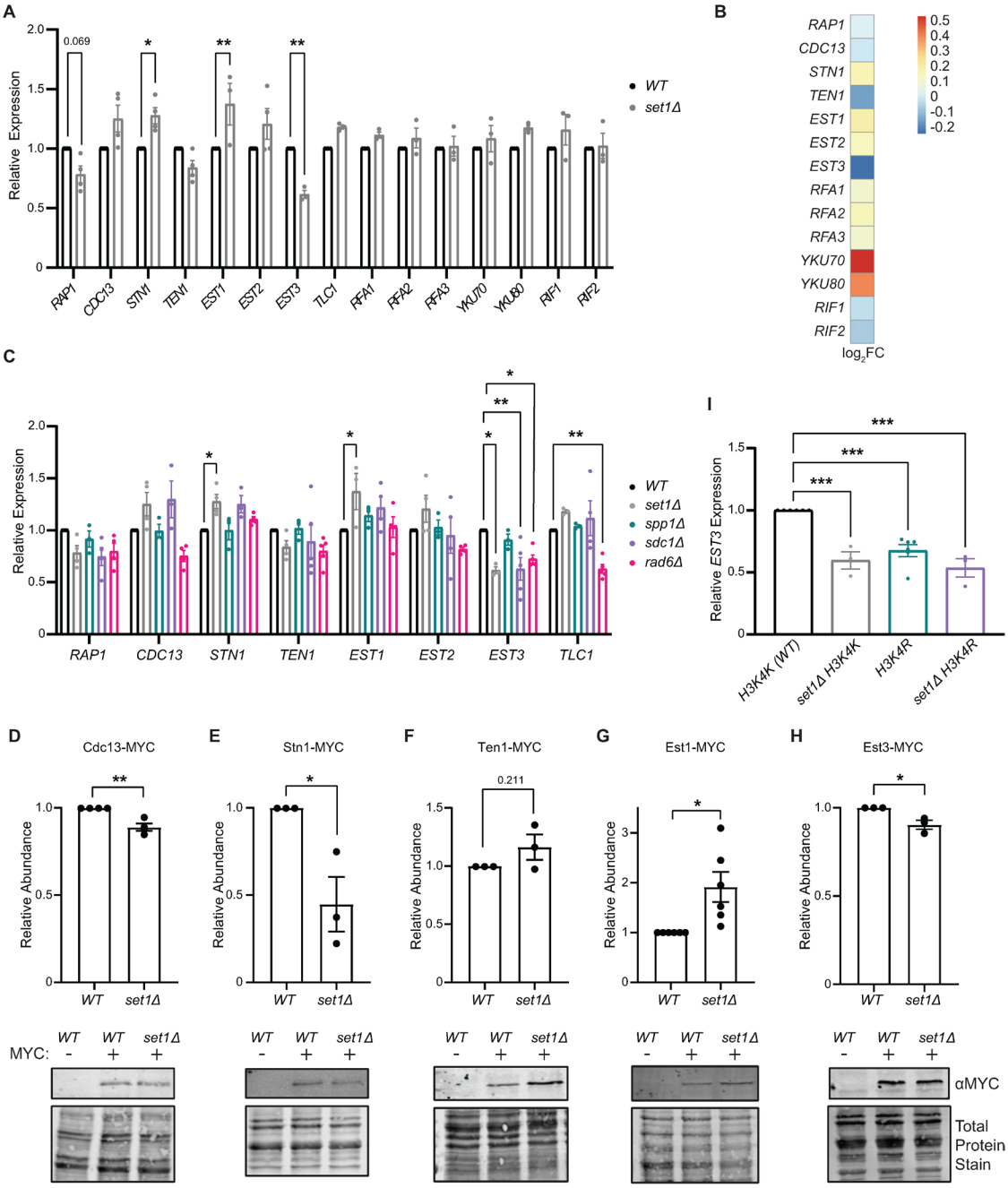

FIGURE 5: Genes encoding telomere maintenance factors show altered abundance levels in *set1*Δ cells. (A) RT-qPCR analysis of genes encoding telomere regulators in *WT* (yEG230) and *set1*Δ (yEG232). Expression was normalized to the control gene *TFC1* and is shown relative to *WT*. Error bars represent SEM for a minimum of three biological replicates. Significance was evaluated using two-way ANOVA and Sidak's multiple comparisons test. (B) Heatmap depicting the log2 fold change of the same telomere maintenance factors shown in A based on previously published RNA-seq data (Jezek *et al.*, 2017a), with the exception of *TLC1*, which was not present in the RNA-seq data. (C) RT-qPCR analysis of genes encoding telomere regulators in *WT* (yEG230), *set1*Δ (yEG232), *spp1*Δ (yEG100), *sdc1*Δ (yEG110), and *rad6*Δ (yEG623). Expression was normalized to the control gene *TFC1* and is shown relative to *WT*. Error bars represent SEM for a minimum of three biological replicates. Significance was evaluated using one-way ANOVA and Tukey's multiple comparisons test for individual genes. (D–H) Quantification of protein abundances of Cdc13-MYC, Stn1-MYC, Ten1-MYC, Est1-MYC, and Est3-MYC in wild-type and *set1*Δ cells. Intensity of MYC signal was determined by Western blot and normalized using a total protein stain as a loading control for a minimum of three biological replicates. Error bars represent SEM. Significance was evaluated using an unpaired *t* test. Representative images of the immunoblots are depicted below each quantification. (I) RT-qPCR analysis of *EST3* in *WT H3K4K* (yEG108), *set1*Δ *H3K4K* (yEG1342), *H3K4R* (yEG109), and *set1*Δ *H3K4R* (yEG1343). Data presented as described for panel A. For all panels, *P* values are indicated as follows: * < 0.05, ** < 0.01, *** < 0.001. All yeast strains described in this figure are derived from the BY4741 background, except strains containing *STN1-MYC* used in panel D and histone mutant strains in panel I (see Supplemental Table S1).

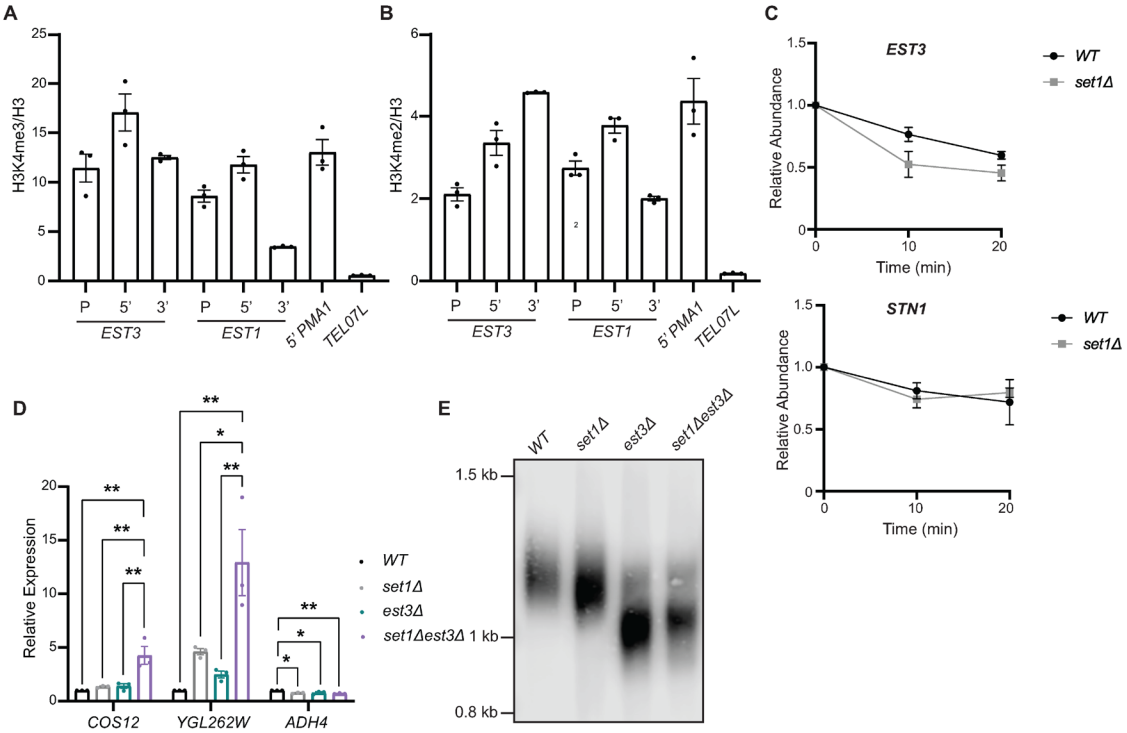

FIGURE 6: Regulation of endogenous *EST3* mRNA and epistasis analysis of *set1*Δ *est3*Δ mutants. chIP of H3K4me3 (A) and H3K4me2 (B) shown relative to total H3 at *EST3* and *EST1* gene loci in *WT* cells (yEG230). Primer sets amplify promoter (P), 5′ coding region (5′), and 3′ coding region (3′). The 5′ coding region of *PMA1* serves as a positive control for H3K4me3/H3K4me2 chromatin localization, and the *TEL07L* region is a negative control. SEM of three biological replicates is shown. (C) Relative abundance of *EST3* and *STN1* mRNAs in *WT* (yEG230) and *set1*Δ (yEG232) cells at 10 and 20 min after thiolutin treatment. *EST3* and *STN1* levels were normalized to the RNA pol II–independent transcript *sCR1*. SEM of three biological replicates is shown. (D) RT-qPCR analysis of *TEL07L* genes in *WT* (yEG1362), *set1*Δ (yEG1363), *est3*Δ (yEG1364), and *set1*Δ *est3*Δ (yEG1365). Expression was normalized to the control gene *TFC1* and is shown relative to *WT*. Error bars represent SEM for a minimum of three biological replicates. Significance was evaluated using two-way ANOVA and Tukey's multiple comparisons test. *P* values are indicated as follows: * < 0.05, ** < 0.01. (E) Southern blot showing terminal telomere fragment molecular weight in *WT* (yEG1362), *set1*Δ (yEG1363), *est3*Δ (yEG1364), and *set1*Δ *est3*Δ (yEG1365). All yeast strains described in this figure are derived from the BY4741 background.

repression and telomere length. Wild-type cells expressing Est3-MYC showed a decrease in subtelomeric gene repression compared with wild-type cells expressing the endogenous untagged Est3, an effect that was further exacerbated in combination with *set1*Δ (Supplemental Figure S4B). We also observed that cells with Est3-MYC have shorter telomeres, approximately equivalent to those of *set1*Δ cells (Supplemental Figure S4C). However, *set1*Δ mutants with *EST3-MYC* show even shorter telomeres than *set1*Δ alone, indicating that each allele is contributing to the short telomere phenotype through a distinct pathway. These data suggest that the *EST3-MYC* allele causes a loss-of-function phenotype due to decreased mRNA abundance and disrupted protein function, and it is not likely to accurately reflect endogenous protein levels of Est3.

Despite the complications in accurately evaluating Est3 protein levels, we next addressed whether Set1 may have a role in transcriptional regulation of *EST3* via the H3K4me3 or H3K4me2 methyl marks. Given that other mutants that show reduced H3K4 methylation also showed lower levels of *EST3* mRNA (Figure 5), we used chromatin immunoprecipitation (chIP) to determine the abundance of H3K4me3 and H3K4me2 at the *EST3* promoter, 5′ ORF and 3′ ORF. We compared this to levels at similar regions of *EST1*, for which the mRNA is increased in the absence of Set1. Both H3K4me3 and H3K4me2 were present to similar extents in the promoters and 5′ ends of *EST3* and *EST1*; however, there was a marked difference at the 3′ end of the ORFs (Figure 6, A and B). Both histone marks, though particularly H3K4me2, showed increased levels at the 3′ end of *EST3* compared with *EST1*. This difference suggests that control of *EST3* mRNA abundance may rely on 3′ deposition of H3K4me2 and that *EST3* regulation may have a greater dependency on H3K4 methylation than *EST1* regulation. This finding is also supported by observations that *sdc1*Δ mutants, but not *spp1*Δ mutants, show increased *EST3* mRNA (Figure 5C).

We also evaluated whether Set1 may regulate posttranscriptional processing or stability of the *EST3* mRNA. In this assay, we compared *EST3* abundance to that of *STN1* because its protein levels appeared decreased by immunoblot despite increased abundance of its mRNA (Figure 5, C and H). Wild-type and *set1*Δ cells were treated with the transcription inhibitor thiolutin, and the mRNA abundance of each transcript was measured by RT-qPCR and compared with that of the RNA pol III–controlled transcript *sCR1*. In this assay, we observed more rapid turnover of the *EST3* transcript in *set1*Δ cells compared with wild type (Figure 6C; *P* value = 0.013 from two-way analysis of variance [ANOVA]), indicating a shorter half-life for the *EST3* mRNA upon loss of Set1. This differed from *STN1*, which showed similar levels in both wild-type and *set1*Δ cells following thiolutin treatment (*P* value = 0.976 from two-way ANOVA), suggesting that each of these transcripts is subject to different regulatory mechanisms dependent on Set1.

Overlapping functions of Set1 and Est3 in telomere maintenance phenotypes

To investigate the dependence of telomere maintenance defects in *set1*Δ on *EST3* expression, we generated *set1*Δ *est3*Δ mutants following sporulation of double heterozygous diploids and evaluated subtelomeric gene repression and telomere length. As expected, both *set1*Δ and *est3*Δ single mutants show increased subtelomeric gene expression (Figure 6D); however, there is a synergistic increase in expression in *set1*Δ *est3*Δ double mutants. These data suggest that both Set1 and Est3 are separately required for subtelomeric gene repression and loss of each of their activities disrupts multiple pathways normally repressing genes within subtelomeric chromatin. Both *set1*Δ and *est3*Δ single mutants also exhibited shorter telomeres (Figure 6E); however, *est3*Δ mutants were much shorter than *set1*Δ mutants. Interestingly, the *set1*Δ *est3*Δ double mutants showed telomere lengths similar to those of *est3*Δ single mutants, indicating that Set1 and Est3 may contribute to the same pathway required for maintaining appropriate telomere lengths. These data suggest that one factor that may contribute to short telomeres in *set1*Δ cells is reduced *EST3* mRNA abundance; however, this is not likely a key contributor to the misregulation of subtelomeric gene repression in the absence of Set1.

DISCUSSION

The lysine methyltransferase Set1 has long been implicated in the regulation of subtelomeric gene repression and telomere length maintenance (Nislow *et al.*, 1997; Corda *et al.*, 1999; Krogan *et al.*, 2002; Schneider *et al.*, 2005; Trelles-Sticken *et al.*, 2005; Jezek *et al.*, 2017a), yet its specific role in these processes has not been completely defined. Based on the association of Set1 and H3K4 methylation with active transcription, the euchromatic distribution of H3K4me3 has been implicated in the maintenance of repressive chromatin at subtelomeres through largely indirect mechanisms (Santos-Rosa *et al.*, 2004; Venkatasubrahmanyam *et al.*, 2007). However, other observations suggest that there are likely additional mechanisms that underlie Set1's role in telomere maintenance pathways. For example, loss of COMPASS components and other factors that deplete H3K4 methyl levels do not always display phenotypes similar to those of *set1*Δ cells (Leung *et al.*, 2011; Wu *et al.*, 2017). In addition, we previously reported that the transcriptome profile of *set1*Δ mutants is most highly correlated with mutants in genes directly linked to telomere maintenance, such as those encoding telomerase subunits (Jezek *et al.*, 2017a). Given these observations, we sought to more systematically define the role for Set1 and H3K4 methylation in two metrics of telomere health: chromatin-mediated gene repression and telomere length.

The Set1 SET domain is required for telomere health through H3K4 methylation–dependent and -independent pathways

Previous studies using reporter assays have suggested that the SET domain of Set1 is primarily responsible for maintaining subtelomeric gene repression (Nislow *et al.*, 1997; Corda *et al.*, 1999); however, the specific contribution of Set1 catalytic methyltransferase activity at H3K4 has been difficult to assess. We used a series of genetic mutations, including the H3K4R point mutation, COMPASS mutants, and mutations in Set1, to quantitatively compare subtelomeric gene expression and simultaneously evaluate telomere length. In a *set1*Δ background, we expressed *FLAG-SET1* from its endogenous promoter on a plasmid and generated multiple point mutations known to abrogate catalytic activity. As loss of catalytic activity is reported to destabilize the Set1 protein (Soares *et al.*, 2014), we monitored abundance of these mutants to clarify whether or not these specific mutations promote Set1 instability. In all mutants tested, we observed decreased levels of FLAG-Set1, indicating that use of these mutants does not provide clean separation of Set1 catalytic and noncatalytic functions.

In addition to catalytic activity localized within the SET domain, Set1 contains two RRMs, which bind a diversity of RNAs (Schlichter and Cairns, 2005; Luciano *et al.*, 2017; Sayou *et al.*, 2017), though whether they contribute to Set1-dependent telomere maintenance had not been directly investigated. Previous studies have also differed on the extent to which H3K4 methylation is affected by loss of the RRM domains (Schlichter and Cairns, 2005; Trésaugues *et al.*, 2006; Luciano *et al.*, 2017). However, our immunoblotting shows equivalent expression of all Set1 mutants tested with moderate loss of H3K4me3 in the RRM deletion mutants, although not in the H422A point mutation that disrupts RNA binding (Trésaugues *et al.*, 2006). This mutant analysis showed that the catalytic core of Set1 is predominantly responsible for maintaining subtelomeric gene repression and telomere length. Interestingly, while the expression of the Set1 catalytic core (Set1 Δ1-761) restores H3K4 methylation levels, the distribution of H3K4me3 and H3K4me2 in the genome is disrupted (Soares *et al.*, 2017). This suggests that specific placement of the H3K4 methyl marks is not required for Set1-dependent telomere maintenance, or that an alternate function of the catalytic core of Set1 may be required. In addition, our analysis of gene expression and telomere length in COMPASS mutants *spp1*Δ and *sdc1*Δ, as well as *rad6*Δ, showed that subtelomeric gene expression changes correlated with the relative loss of H3K4 methyl species in these mutants. However, this was not the case for telomere length, which showed little change from wild type in all of these mutants. These findings indicate that telomere length maintenance and repression of subtelomeric chromatin are separable processes that show differential requirements for H3K4 methylation.

In addition to catalyzing H3K4 methylation, the SET domain of Set1 has additional functions. Set1 methylates the kinetochore-associated protein Dam1 (Zhang *et al.*, 2005), and more recently, H3K37me1 has been reported to be targeted by Set1 together with the H3K36 methyltransferase Set2 (Santos-Rosa *et al.*, 2021). In a noncatalytic role, the SET domain of Set1 physically interacts with the DNA damage protein Mec3 (Corda *et al.*, 1999), which may also contribute to its function at telomeres. Furthermore, orthologues of Set1 have been shown to perform functions independent of the catalytic methyltransferase activity (Kirmizis *et al.*, 2007; Dorighi *et al.*, 2017; Rickels *et al.*, 2017, 2020). Further identification of mutants that separate functions of the SET domain is needed to better define the specific contributions of catalytic and noncatalytic activities to Set1's role in telomere maintenance, as well as its other biological roles.

Altered abundance of telomere maintenance factors in *set1*Δ mutants through transcriptional and posttranscriptional regulation

To better define the role of Set1 in telomere maintenance, we assayed steady-state mRNA and protein abundance of a series of telomere regulators in cells lacking Set1, Spp1, Sdc1, or Rad6, with a focus on components of the CST telomere capping complex and the telomerase holoenzyme. At the mRNA level, we observed alterations to the abundance of *STN1*, *TEN1*, *EST1*, *EST3*, and *TLC1*. There appeared to be an enhanced dependence on H3K4me2 or H3K4me1 for regulating mRNA abundance, as *sdc1*Δ mutants most closely mimicked *set1*Δ cells. Interestingly, in monitoring protein abundance of these factors, we observed that the mRNA and

protein levels change in parallel for some factors, such as Est1; however, some proteins displayed changes in abundance that could not be explained by changes at the mRNA level. For example, *STN1* transcript levels are increased in *set1*Δ, while Stn1-MYC was decreased. This is also seen, albeit to a lesser extent, with Cdc13, whose transcript levels increased in *set1*Δ cells while the protein abundance was slightly reduced. This suggests altered translational or posttranslational regulation of CST components in the absence of Set1. Both Cdc13 and Stn1 are subject to posttranslational regulation: they are phosphorylated by the cyclin-dependent kinase, Cdk1, and this modification serves to stabilize the complex at the telomere (Tseng *et al.*, 2009; Liu *et al.*, 2014; Gopalakrishnan *et al.*, 2017). This phosphorylation, and possibly other regulatory mechanisms including transcriptional control, may be disrupted in *set1*Δ cells due to their aberrant cell cycle progression (Beilharz *et al.*, 2017). The abundance and stoichiometry of CST complex components is exquisitely regulated in the cell, and previous work has identified multiple mechanisms of regulation and shown that alterations to any of the complex members can impact telomere function and promote feedback regulation of other telomere maintenance factors (Morris and Lundblad, 1997; Enomoto *et al.*, 2004; Larose *et al.*, 2007; Tuzon *et al.*, 2011; Advani *et al.*, 2013; Holstein *et al.*, 2014; Liu *et al.*, 2014; Tucey and Lundblad, 2014; Cesena *et al.*, 2017; Gopalakrishnan *et al.*, 2017; Mersaoui and Wellinger, 2019; Garcia *et al.*, 2020). Our data indicate that Set1 promotes the proper balance of CST components within the cell and this disruption in *set1*Δ cells likely contributes to impaired telomere function.

In addition to altered abundance of CST factors, we noted differential abundance of *EST1* and *EST3* mRNAs, each of which encodes components of the telomerase holoenzyme. The increase in *EST1* in *set1*Δ cells was reflected in higher abundance of the Est1-MYC protein. The enrichment of H3K4me3 and H3K4me2 at the *EST1* gene suggests that it may be subject to Set1-dependent transcriptional regulation; however, other mechanisms controlling protein abundance may also be disrupted in the absence of Set1. For example, Est1 protein levels are regulated posttranslationally through a proteasome-dependent process involving the ubiquitin ligase Ufd4 and the ubiquitin-binding complex Cdc48-Npl4-Ufd1 (Lin *et al.*, 2015). Further experiments are required to determine the relative contribution of these mechanisms to controlling Est1 abundance.

At the transcript level, *EST3* showed the largest change in abundance in *set1*Δ cells and related mutants. This is consistent with our previous findings that the transcriptome in *set1*Δ cells is highly correlated with that of *est3*Δ mutants (Jezek *et al.*, 2017a). Further analysis of the *EST3* mRNA half-life following thiolutin treatment indicated more rapid degradation of *EST3* mRNA than that of *STN1*, suggesting that *EST3* posttranscriptional regulation is disrupted in the absence of Set1. Interestingly, the *EST3* mRNA undergoes programmed ribosomal frameshifting and is regulated by the nonsense mediated decay (NMD) pathway (Morris and Lundblad, 1997; Enomoto *et al.*, 2004). One possibility is that there is increased shunting of the *EST3* mRNA to the NMD pathway in *set1*Δ cells, potentially through misregulated frameshifting or other processing or translation defect.

We investigated Est3 protein abundance in *set1*Δ cells by integrating a MYC tag at the C-terminus, as there is no available antibody for detecting Est3. It has previously been reported that C-terminal epitope tags can disrupt function of Est3 (Tuzon *et al.*, 2011; Tucey and Lundblad, 2014). Indeed, we observed decreased gene repression and shorter telomeres with the addition of the C-terminal MYC tag, though also a substantial decrease in mRNA abundance. While we could not conclusively determine whether full-length Est3 protein showed decreased abundance in *set1*Δ cells, epistasis analysis of *set1*Δ *est3*Δ double mutants suggested that Set1 and Est3 contribute separately to subtelomeric gene repression. However, *set1*Δ *est3*Δ cells have telomere lengths similar to those of *est3*Δ single mutants, indicating that Set1 and Est3 both contribute to the same pathway to maintain telomere length.

In summary, our data indicate that Set1's role at telomeres depends on the activity of its catalytic core, although H3K4 methylation–independent functions likely contribute to telomere length maintenance. The role for Set1 in subtelomeric gene repression is most closely correlated with H3K4 methyl status, indicating that this mark is required for gene repression and, further, that misregulated subtelomeric chromatin is not the primary driver of telomere shortening in *set1*Δ mutants. These differential requirements for H3K4 methylation are also evident in our analysis of mRNA abundance of telomere maintenance factors, with genes such as *EST3* likely dependent on H3K4 methyl status for regulation, but not *EST1* or *STN1*. These transcripts show disrupted transcriptional and posttranscriptional regulation in the absence of Set1, as well as possible translational or posttranslational mechanisms directing protein abundance. This likely reflects the multiple mechanisms that precisely calibrate the abundance of these critical telomere regulators. Altogether, this study provides new and unexpected insights into how Set1 promotes telomeric and subtelomeric function and provides the foundation for dissecting the roles of H3K4 methyl species and additional targets of Set1 in telomere maintenance pathways in yeast and other systems.

MATERIALS AND METHODS

Request a protocol through *Bio-protocol*.

Yeast strains and growth conditions

Yeast strains, plasmids, and primers used in this study are listed in Supplemental Tables S1, S2, and S3, respectively. Gene knockouts, incorporation of epitope tags, and plasmid construction and transformation were performed using standard methods (Longtine *et al.*, 1998; Jaiswal *et al.*, 2017; Jezek *et al.*, 2017b; Tran *et al.*, 2018; Jaiswal *et al.*, 2020). The *FLAG-SET1* allele was constructed by targeting of a 2xFLAG-containing PCR cassette upstream of the *SET1* coding sequence, as described (Moqtaderi and Struhl, 2008). This sequence was PCR-amplified from genomic DNA, along with the *SET1* promoter and 3′UTR, and cloned into pRS316 for generating mutants in a plasmid-based expression system. Amino acid substitutions and domain deletions were made using either Gibson assembly or the Q5 Site-Directed Mutagenesis Kit (NEB). Isogenic single and double mutant strains were generated via haploid mating, sporulation, and tetrad dissection. Genotypes were confirmed using PCR (endogenous mutations) or plasmid sequencing. Standard liquid and solid growth media were used (yeast extract, peptone, dextrose [YPD] and synthetic complete [SC]-dropout). The *CDC13* temperature-sensitive mutant strain was a gift from David Lydall (Newcastle University) (Holstein *et al.*, 2014).

RNA extraction and RT-qPCR to measure mRNA abundance

RNA was extracted from 1.5 ml of logarithmically growing cells (OD_{600} ~0.6–0.8) using the Masterpure Yeast RNA Purification kit (Epicentre). Residual genomic DNA was removed using the Turbo DNA-free kit (Ambion). cDNA was synthesized using the qMax cDNA Synthesis Kit (Accuris) with 1 µg of template RNA. qPCR was performed to assess mRNA transcript levels with qMax Green Low Rox qPCR Mix (Accuris), 0.5 µl of cDNA, and 20 µM forward and

reverse gene specific primers. Amplification was performed using the CFX384 Real-time Detection System (Bio-Rad). Each reaction was performed in technical triplicate and a minimum of three biological replicates. mRNA abundance was determined relative to the control gene *TFC1* and displayed as fold change (or relative expression) compared with wild type. To measure mRNA degradation, cells were treated with 10 µg/ml thiolutin (ENZO Life Sciences) and harvested at 10 and 20 min after treatment. mRNA abundance was determined relative to the control gene *sCR1* and normalized to the zero time point. All qPCR primers used are listed in Supplemental Table S3.

DNA preparation and Southern blots of telomere length

Telomere length was assessed using a nonradioactive Southern blotting protocol (Feng *et al.*, 2013). Briefly, 10 ml of yeast culture was grown overnight at 30°C and harvested. Pellets were resuspended in yeast breaking buffer (10 mM Tris-HCl, pH 8.0, 100 mM NaCl, 1 mM EDTA, pH 8.0, 1% SDS, 2% Triton X-100) and vortexed with acid-washed glass beads (Sigma-Aldrich) with phenol–chloroform–isoamyl alcohol (PCI; 25:24:1) (VWR Scientific). After centrifugation, DNA was isolated from the supernatant via ethanol precipitation and treated with RNaseA. Genomic DNA was digested with *Xho*I (NEB) and subject to PCI extraction and ethanol precipitation. Prepared DNA (40–60 µg) was loaded onto an 0.8% agarose gel (0.5% tris borate EDTA [TBE]) and run for 25 h at 100 V. Ethidium bromide staining and imaging was used to observe DNA migration. Following denaturation and washing (Feng *et al.*, 2013), DNA was transferred onto an N+hybond membrane (Amersham) before cross-linking. The blot was probed with 15 ng/ml biotinylated telomere probe (5′-biotin-CACACCCACACCCACACC-3′) at 65°C overnight. Nucleic acids on the blot were detected using a Chemiluminescent Nucleic Acid Detection Module Kit (ThermoFisher) per the manufacturer's instructions and imaged using a LiCor C-Digit chemiluminescence imager.

Yeast senescence assays

To obtain replicatively "young" cells for all appropriate genotypes, tetrad dissections of heterozygous diploid strains were used to generate isogenic haploid strains. Senescence assays were performed as described (Kozak *et al.*, 2010; Lu and Liu, 2010). Briefly, cells were grown on plates for 3 d and single colonies were used to inoculate 10 ml of YPD. The cells were grown overnight with shaking at 30°C. Cell density was calculated using a hemocytometer, and new cultures were diluted to 1×10^4 cells/ml from the overnight cultures. After 24 h, cell density was recorded and new cultures were inoculated at 1×10^4 cells/ml. This procedure was repeated every 24 h for up to 15 d. The number of population doublings per culture was calculated for each time point taken. Experiments were performed in biological triplicate.

Yeast spot assays

Cells were grown at 30°C to saturation in 5 ml of YPD and then diluted to 1.0 OD_{600} units. Tenfold serial dilutions were plated on the appropriate media, including YPD, SC-URA, SC-URA + 100 mM hydroxyurea, or SC-URA + 10 mM caffeine. For temperature sensitivity assays, plates were grown at the indicated temperatures and imaged up to 4 d. For DNA damage sensitivity assays, plates were grown at 30°C and imaged daily for up to 7 d.

Immunoblotting

Lysates for immunoblotting were prepared using either 0.2 M NaOH treatment or bead-beating in lysis buffer (50 mM Tris-HCl, pH 7.5, 150 mM NaCl, 1 mM EDTA, 1% NP-40) (Jezek *et al.*, 2017a; Tran *et al.*, 2018). Protein concentrations were determined by Bradford assay and normalized to load equivalent amounts on SDS–PAGE. Proteins were transferred to Immobilon-FL polyvinylidene difluoride membrane (Fisher Scientific). Blots were probed overnight with primary antibodies, followed by incubation with the appropriate secondary antibody. Blots were imaged using an Odyssey CLx Scanner and processed using ImageStudio (LiCor). Total Protein Stain (LiCor) was used to determine total protein amounts for quantitation. Antibodies used in this study were c-MYC 9E10 (Novus Biologicals NB600-302SS), monoclonal anti-FLAG M2 (Sigma-Aldrich F1804), H3K4me3 (Active Motif 39159), H3K4me2 (Active Motif 39142), H3 (Abcam ab1791), H4 (Abcam ab31830), IRDye 680RD goat anti-mouse immunoglobulin G (IgG) (LiCor 926-68070), and IRDye 800CW goat anti-rabbit IgG (LiCor 926-32211).

Chromatin immunoprecipitation

chIP was performed as previously described (Jezek *et al.*, 2017a,b; Jethmalani *et al.*, 2021). All primers used for amplification of chromatin regions are listed in Supplemental Table S3. The ratio of percent input for the histone mark (H3K4me3 or H3K4me2) is shown relative to percent input for histone H3.

ACKNOWLEDGMENTS

We thank all members of the Green lab for helpful discussions, technical assistance, and feedback on the manuscript. We thank David Lydall for yeast strains and Philip Farabaugh for sharing equipment. This work was supported by National Institutes of Health (NIH) R01GM124342 to E.M.G. M.Y.N. was supported by funds from NIH T32GM055036 and R25GM066706 and National Science Foundation LSAMP BD 1500511 to the University of Maryland Baltimore County. The content is solely the responsibility of the authors and does not necessarily represent the official views of the National Institutes of Health.

REFERENCES

Advani VM, Belew AT, Dinman JD (2013). Yeast telomere maintenance is globally controlled by programmed ribosomal frameshifting and the nonsense-mediated mRNA decay pathway. Translation (Austin) 1, e24418.

Beilharz TH, Harrison PF, Miles DM, See MM, Le UM, Kalanon M, Curtis MJ, Hasan Q, Saksouk J, Margaritis T, *et al.* (2017). Coordination of cell cycle progression and mitotic spindle assembly involves histone H3 lysine 4 methylation by Set1/COMPASS. Genetics 205, 185–199.

Bernstein BE, Humphrey EL, Erlich RL, Schneider R, Bouman P, Liu JS, Kouzarides T, Schreiber SL (2002). Methylation of histone H3 Lys 4 in coding regions of active genes. Proc Natl Acad Sci USA 99, 8695–8700.

Berretta J, Pinskaya M, Morillon A (2008). A cryptic unstable transcript mediates transcriptional trans-silencing of the Ty1 retrotransposon in S. cerevisiae. Genes Dev 22, 615–626.

Briggs SD, Bryk M, Strahl BD, Cheung WL, Davie JK, Dent SY, Winston F, Allis CD (2001). Histone H3 lysine 4 methylation is mediated by Set1 and required for cell growth and rDNA silencing in Saccharomyces cerevisiae. Genes Dev 15, 3286–3295.

Bryk M, Briggs SD, Strahl BD, Curcio MJ, Allis CD, Winston F (2002). Evidence that Set1, a factor required for methylation of histone H3, regulates rDNA silencing in S. cerevisiae by a Sir2-independent mechanism. Curr Biol 12, 165–170.

Castelnuovo M, Zaugg JB, Guffanti E, Maffioletti A, Camblong J, Xu Z, Clauder-Münster S, Steinmetz LM, Luscombe NM, Stutz F (2014). Role of histone modifications and early termination in pervasive transcription and antisense-mediated gene silencing in yeast. Nucleic Acids Res 42, 4348–4362.

Cesena D, Cassani C, Rizzo E, Lisby M, Bonetti D, Longhese MP (2017). Regulation of telomere metabolism by the RNA processing protein Xrn1. Nucleic Acids Res 45, 3860–3874.

Corda Y, Schramke V, Longhese MP, Smokvina T, Paciotti V, Brevet V, Gilson E, Géli V (1999). Interaction between Set1p and checkpoint protein Mec3p in DNA repair and telomere functions. Nat Genet 21, 204–208.
Cruz C, Della Rosa M, Krueger C, Gao Q, Horkai D, King M, Field L, Houseley J (2018). Tri-methylation of histone H3 lysine 4 facilitates gene expression in ageing cells. eLife 7, e34081.
Dehé PM, Dichtl B, Schaft D, Roguev A, Pamblanco M, Lebrun R, Rodríguez-Gil A, Mkandawire M, Landsberg K, Shevchenko A, *et al*. (2006). Protein interactions within the Set1 complex and their roles in the regulation of histone 3 lysine 4 methylation. J Biol Chem 281, 35404–35412.
Dehé PM, Pamblanco M, Luciano P, Lebrun R, Moinier D, Sendra R, Verreault A, Tordera V, Géli V (2005). Histone H3 lysine 4 mono-methylation does not require ubiquitination of histone H2B. J Mol Biol 353, 477–484.
de La Roche Saint-André C, Géli V (2021). Set1-dependent H3K4 methylation becomes critical for limiting DNA damage in response to changes in S-phase dynamics in Saccharomyces cerevisiae. DNA Repair (Amst) 105, 103159.
Dorighi KM, Swigut T, Henriques T, Bhanu NV, Scruggs BS, Nady N, Still CD, Garcia BA, Adelman K, Wysocka J (2017). Mll3 and Mll4 facilitate enhancer RNA synthesis and transcription from promoters independently of H3K4 monomethylation. Mol Cell 66, 568–576.e564.
Ellahi A, Thurtle DM, Rine J (2015). The chromatin and transcriptional landscape of native Saccharomyces cerevisiae telomeres and subtelomeric domains. Genetics 200, 505–521.
Enomoto S, Glowczewski L, Lew-Smith J, Berman JG (2004). Telomere cap components influence the rate of senescence in telomerase-deficient yeast cells. Mol Cell Biol 24, 837–845.
Faucher D, Wellinger RJ (2010). Methylated H3K4, a transcription-associated histone modification, is involved in the DNA damage response pathway. PLoS Genet 6, e1001082.
Feng X, Luo Z, Jiang S, Li F, Han X, Hu Y, Wang D, Zhao Y, Ma W, Liu D, *et al*. (2013). The telomere-associated homeobox-containing protein TAH1/HMBOX1 participates in telomere maintenance in ALT cells. J Cell Sci 126, 3982–3989.
Garcia PD, Leach RW, Wadsworth GM, Choudhary K, Li H, Aviran S, Kim HD, Zakian VA (2020). Stability and nuclear localization of yeast telomerase depend on protein components of RNase P/MRP. Nat Commun 11, 2173.
Gopalakrishnan V, Tan CR, Li S (2017). Sequential phosphorylation of CST subunits by different cyclin-Cdk1 complexes orchestrate telomere replication. Cell Cycle 16, 1271–1287.
Holstein EM, Clark KR, Lydall D (2014). Interplay between nonsense-mediated mRNA decay and DNA damage response pathways reveals that Stn1 and Ten1 are the key CST telomere-cap components. Cell Rep 7, 1259–1269.
Jaiswal D, Jezek M, Quijote J, Lum J, Choi G, Kulkarni R, Park D, Green EM (2017). Repression of middle sporulation genes in *Saccharomycescerevisiae* by the Sum1-Rfm1-Hst1 complex is maintained by Set1 and H3K4 methylation. G3 (Bethesda) 7, 3971–3982.
Jaiswal D, Turniansky R, Moresco JJ, Ikram S, Ramaprasad G, Akinwole A, Wolf J, Yates JR, Green EM (2020). Function of the MYND domain and C-terminal region in regulating the subcellular localization and catalytic activity of the SMYD family lysine methyltransferase Set5. Mol Cell Biol 40, e00341–19.
Jethmalani Y, Tran K, Negesse MY, Sun W, Ramos M, Jaiswal D, Jezek M, Amos S, Garcia EJ, Park D, Green EM (2021). Set4 regulates stress response genes and coordinates histone deacetylases within yeast subtelomeres. Life Sci Alliance 4, e2021101126.
Jezek M, Gast A, Choi G, Kulkarni R, Quijote J, Graham-Yooll A, Park D, Green EM (2017a). The histone methyltransferases Set5 and Set1 have overlapping functions in gene silencing and telomere maintenance. Epigenetics 12, 93–104.
Jezek M, Green EM (2019). Histone modifications and the maintenance of telomere integrity. Cells 8, 199.
Jezek M, Jacques A, Jaiswal D, Green EM (2017b). Chromatin immunoprecipitation (ChIP) of histone modifications from Saccharomyces cerevisiae. J Vis Exp 130, 57080.
Kim J, Kim JA, McGinty RK, Nguyen UT, Muir TW, Allis CD, Roeder RG (2013). The n-SET domain of Set1 regulates H2B ubiquitylation-dependent H3K4 methylation. Mol Cell 49, 1121–1133.
Kirmizis A, Santos-Rosa H, Penkett CJ, Singer MA, Vermeulen M, Mann M, Bähler J, Green RD, Kouzarides T (2007). Arginine methylation at histone H3R2 controls deposition of H3K4 trimethylation. Nature 449, 928–932.
Kozak ML, Chavez A, Dang W, Berger SL, Ashok A, Guo X, Johnson FB (2010). Inactivation of the Sas2 histone acetyltransferase delays senescence driven by telomere dysfunction. EMBO J 29, 158–170.
Krogan NJ, Dover J, Khorrami S, Greenblatt JF, Schneider J, Johnston M, Shilatifard A (2002). COMPASS, a histone H3 (lysine 4) methyltransferase required for telomeric silencing of gene expression. J Biol Chem 277, 10753–10755.
Kupiec M (2014). Biology of telomeres: lessons from budding yeast. FEMS Microbiol Rev 38, 144–171.
Larose S, Laterreur N, Ghazal G, Gagnon J, Wellinger RJ, Elela SA (2007). RNase III-dependent regulation of yeast telomerase. J Biol Chem 282, 4373–4381.
Lee JS, Shukla A, Schneider J, Swanson SK, Washburn MP, Florens L, Bhaumik SR, Shilatifard A (2007). Histone crosstalk between H2B monoubiquitination and H3 methylation mediated by COMPASS. Cell 131, 1084–1096.
Lenstra TL, Benschop JJ, Kim T, Schulze JM, Brabers NA, Margaritis T, van de Pasch LA, van Heesch SA, Brok MO, Groot Koerkamp MJ, *et al*. (2011). The specificity and topology of chromatin interaction pathways in yeast. Mol Cell 42, 536–549.
Leung A, Cajigas I, Jia P, Ezhkova E, Brickner JH, Zhao Z, Geng F, Tansey WP (2011). Histone H2B ubiquitylation and H3 lysine 4 methylation prevent ectopic silencing of euchromatic loci important for the cellular response to heat. Mol Biol Cell 22, 2741–2753.
Lin KW, McDonald KR, Guise AJ, Chan A, Cristea IM, Zakian VA (2015). Proteomics of yeast telomerase identified Cdc48-Npl4-Ufd1 and Ufd4 as regulators of Est1 and telomere length. Nat Commun 6, 8290.
Liu CC, Gopalakrishnan V, Poon LF, Yan T, Li S (2014). Cdk1 regulates the temporal recruitment of telomerase and Cdc13-Stn1-Ten1 complex for telomere replication. Mol Cell Biol 34, 57–70.
Longtine MS, McKenzie A, Demarini DJ, Shah NG, Wach A, Brachat A, Philippsen P, Pringle JR (1998). Additional modules for versatile and economical PCR-based gene deletion and modification in Saccharomyces cerevisiae. Yeast 14, 953–961.
Lu J, Liu Y (2010). Deletion of Ogg1 DNA glycosylase results in telomere base damage and length alteration in yeast. EMBO J 29, 398–409.
Luciano P, Jeon J, El-Kaoutari A, Challal D, Bonnet A, Barucco M, Candelli T, Jourquin F, Lesage P, Kim J, *et al*. (2017). Binding to RNA regulates Set1 function. Cell Discov 3, 17040.
Margaritis T, Oreal V, Brabers N, Maestroni L, Vitaliano-Prunier A, Benschop JJ, van Hooff S, van Leenen D, Dargemont C, Géli V, Holstege FC (2012). Two distinct repressive mechanisms for histone 3 lysine 4 methylation through promoting 3′-end antisense transcription. PLoS Genet 8, e1002952.
Martín GM, King DA, Green EM, Garcia-Nieto PE, Alexander R, Collins SR, Krogan NJ, Gozani OP, Morrison AJ (2014). Set5 and Set1 cooperate to repress gene expression at telomeres and retrotransposons. Epigenetics 9, 513–522.
Mersaoui SY, Wellinger RJ (2019). Fine tuning the level of the Cdc13 telomere-capping protein for maximal chromosome stability performance. Curr Genet 65, 109–118.
Miller T, Krogan NJ, Dover J, Erdjument-Bromage H, Tempst P, Johnston M, Greenblatt JF, Shilatifard A (2001). COMPASS: a complex of proteins associated with a trithorax-related SET domain protein. Proc Natl Acad Sci USA 98, 12902–12907.
Moqtaderi Z, Struhl K (2008). Expanding the repertoire of plasmids for PCR-mediated epitope tagging in yeast. Yeast 25, 287–292.
Morris DK, Lundblad V (1997). Programmed translational frameshifting in a gene required for yeast telomere replication. Curr Biol 7, 969–976.
Nagy PL, Griesenbeck J, Kornberg RD, Cleary ML (2002). A trithorax-group complex purified from Saccharomyces cerevisiae is required for methylation of histone H3. Proc Natl Acad Sci USA 99, 90–94.
Ng HH, Dole S, Struhl K (2003). The Rtf1 component of the Paf1 transcriptional elongation complex is required for ubiquitination of histone H2B. J Biol Chem 278, 33625–33628.
Nislow C, Ray E, Pillus L (1997). SET1, a yeast member of the trithorax family, functions in transcriptional silencing and diverse cellular processes. Mol Biol Cell 8, 2421–2436.
Pokholok DK, Harbison CT, Levine S, Cole M, Hannett NM, Lee TI, Bell GW, Walker K, Rolfe PA, Herbolsheimer E, *et al*. (2005). Genome-wide map of nucleosome acetylation and methylation in yeast. Cell 122, 517–527.
Ramakrishnan S, Pokhrel S, Palani S, Pflueger C, Parnell TJ, Cairns BR, Bhaskara S, Chandrasekharan MB (2016). Counteracting H3K4 methylation modulators Set1 and Jhd2 co-regulate chromatin dynamics and gene transcription. Nat Commun 7, 11949.

Rickels R, Herz HM, Sze CC, Cao K, Morgan MA, Collings CK, Gause M, Takahashi YH, Wang L, Rendleman EJ, *et al*. (2017). Histone H3K4 monomethylation catalyzed by Trr and mammalian COMPASS-like proteins at enhancers is dispensable for development and viability. Nat Genet 49, 1647–1653.

Rickels R, Wang L, Iwanaszko M, Ozark PA, Morgan MA, Piunti A, Khalatyan N, Soliman SHA, Rendleman EJ, Savas JN, *et al*. (2020). A small UTX stabilization domain of Trr is conserved within mammalian MLL3-4/COMPASS and is sufficient to rescue loss of viability in null animals. Genes Dev 34, 1493–1502.

Roguev A, Schaft D, Shevchenko A, Pijnappel WW, Wilm M, Aasland R, Stewart AF (2001). The Saccharomyces cerevisiae Set1 complex includes an Ash2 homologue and methylates histone 3 lysine 4. EMBO J 20, 7137–7148.

Santos-Rosa H, Bannister AJ, Dehe PM, Géli V, Kouzarides T (2004). Methylation of H3 lysine 4 at euchromatin promotes Sir3p association with heterochromatin. J Biol Chem 279, 47506–47512.

Santos-Rosa H, Millán-Zambrano G, Han N, Leonardi T, Klimontova M, Nasiscionyte S, Pandolfini L, Tzelepis K, Bartke T, Kouzarides T (2021). Methylation of histone H3 at lysine 37 by Set1 and Set2 prevents spurious DNA replication. Mol Cell 81, 2793–2807.e2798.

Santos-Rosa H, Schneider R, Bannister AJ, Sherriff J, Bernstein BE, Emre NC, Schreiber SL, Mellor J, Kouzarides T (2002). Active genes are tri-methylated at K4 of histone H3. Nature 419, 407–411.

Sayou C, Millán-Zambrano G, Santos-Rosa H, Petfalski E, Robson S, Houseley J, Kouzarides T, Tollervey D (2017). RNA binding by histone methyltransferases Set1 and Set2. Mol Cell Biol 37, e00165–16.

Schlichter A, Cairns BR (2005). Histone trimethylation by Set1 is coordinated by the RRM, autoinhibitory, and catalytic domains. EMBO J 24, 1222–1231.

Schneider J, Wood A, Lee JS, Schuster R, Dueker J, Maguire C, Swanson SK, Florens L, Washburn MP, Shilatifard A (2005). Molecular regulation of histone H3 trimethylation by COMPASS and the regulation of gene expression. Mol Cell 19, 849–856.

Soares LM, He PC, Chun Y, Suh H, Kim T, Buratowski S (2017). Determinants of histone H3K4 methylation patterns. Mol Cell 68, 773–785.e776.

Soares LM, Radman-Livaja M, Lin SG, Rando OJ, Buratowski S (2014). Feedback control of Set1 protein levels is important for proper H3K4 methylation patterns. Cell Rep 6, 961–972.

Sun ZW, Allis CD (2002). Ubiquitination of histone H2B regulates H3 methylation and gene silencing in yeast. Nature 418, 104–108.

Tran K, Jethmalani Y, Jaiswal D, Green EM (2018). Set4 is a chromatin-associated protein, promotes survival during oxidative stress, and regulates stress response genes in yeast. J Biol Chem 293, 14429–14443.

Trelles-Sticken E, Bonfils S, Sollier J, Géli V, Scherthan H, de La Roche Saint-André C (2005). Set1- and Clb5-deficiencies disclose the differential regulation of centromere and telomere dynamics in Saccharomyces cerevisiae meiosis. J Cell Sci 118, 4985–4994.

Trésaugues L, Dehé PM, Guérois R, Rodriguez-Gil A, Varlet I, Salah P, Pamblanco M, Luciano P, Quevillon-Cheruel S, Sollier J, *et al*. (2006). Structural characterization of Set1 RNA recognition motifs and their role in histone H3 lysine 4 methylation. J Mol Biol 359, 1170–1181.

Tseng SF, Shen ZJ, Tsai HJ, Lin YH, Teng SC (2009). Rapid Cdc13 turnover and telomere length homeostasis are controlled by Cdk1-mediated phosphorylation of Cdc13. Nucleic Acids Res 37, 3602–3611.

Tucey TM, Lundblad V (2014). Regulated assembly and disassembly of the yeast telomerase quaternary complex. Genes Dev 28, 2077–2089.

Tuzon CT, Wu Y, Chan A, Zakian VA (2011). The Saccharomyces cerevisiae telomerase subunit Est3 binds telomeres in a cell cycle- and Est1-dependent manner and interacts directly with Est1 in vitro. PLoS Genet 7, e1002060.

Venkatasubrahmanyam S, Hwang WW, Meneghini MD, Tong AH, Madhani HD (2007). Genome-wide, as opposed to local, antisilencing is mediated redundantly by the euchromatic factors Set1 and H2A.Z. Proc Natl Acad Sci USA 104, 16609–16614.

Weiner A, Chen HV, Liu CL, Rahat A, Klien A, Soares L, Gudipati M, Pfeffner J, Regev A, Buratowski S, *et al*. (2012). Systematic dissection of roles for chromatin regulators in a yeast stress response. PLoS Biol 10, e1001369.

Wellinger RJ, Zakian VA (2012). Everything you ever wanted to know about Saccharomyces cerevisiae telomeres: beginning to end. Genetics 191, 1073–1105.

Wu Z, Liu J, Zhang QD, Lv DK, Wu NF, Zhou JQ (2017). Rad6-Bre1-mediated H2B ubiquitination regulates telomere replication by promoting telomere-end resection. Nucleic Acids Res 45, 3308–3322.

Zhang K, Lin W, Latham JA, Riefler GM, Schumacher JM, Chan C, Tatchell K, Hawke DH, Kobayashi R, Dent SY (2005). The Set1 methyltransferase opposes Ipl1 aurora kinase functions in chromosome segregation. Cell 122, 723–734.

Zhang W, Bone JR, Edmondson DG, Turner BM, Roth SY (1998). Essential and redundant functions of histone acetylation revealed by mutation of target lysines and loss of the Gcn5p acetyltransferase. EMBO J 17, 3155–3167.

ETOC:

Set1 regulates subtelomeric gene repression and telomere length via H3K4 methylation–dependent and -independent pathways, respectively. Set1 and H3K4 methylation also control the abundance of components of the telomerase holoenzyme and the CST complex.